

Structural evolution and magnetic properties of $ScLi_n$ (n=2-13) clusters: A PSO and DFT investigation

Lu Li(栗潞), Xiu-Hua Cui(崔秀花), Hai-Bin Cao(曹海宾), Yi Jiang(姜轶), Hai-Ming Duan(段海明), Qun Jing(井群), Jing Liu(刘静), Qian Wang(王倩)

Citation: Chin. Phys. B . 2020, 29(7): 077101 . **doi:** 10.1088/1674-1056/ab8d9e
Journal homepage: http://cpb.iphy.ac.cn; http://iopscience.iop.org/cpb

What follows is a list of articles you may be interested in

Ab initio study of structural, electronic, thermo-elastic and optical properties of Pt_3Zr intermetallic compound

Wahiba Metiri, Khaled Cheikh

Chin. Phys. B . 2020, 29(4): 047101 . **doi:** 10.1088/1674-1056/ab7223

A simple rule for finding Dirac cones in bilayered perovskites

Xuejiao Chen(陈雪娇), Lei Liu(刘雷), Dezhen Shen(申德振)

Chin. Phys. B . 2019, 28(7): 077106 . **doi:** 10.1088/1674-1056/28/7/077106

Theoretical design of multifunctional half-Heusler materials based on first-principles calculations

Xiuwen Zhang(张秀文)

Chin. Phys. B . 2018, 27(12): 127101 . **doi:** 10.1088/1674-1056/27/12/127101

Band structure engineering and defect control of oxides for energy applications

Hui-Xiong Deng(邓惠雄), Jun-Wei Luo(骆军委), Su-Huai Wei(魏苏淮)

Chin. Phys. B . 2018, 27(11): 117104 . **doi:** 10.1088/1674-1056/27/11/117104

First principles study of stability, mechanical, and electronic properties of chromium silicides

Bo Ren(任博), De-Hong Lu(卢德宏), Rong Zhou(周荣), De-Peng Ji(姬德朋), Ming-Yu Hu(胡明钰), Jing Feng(冯晶)

Chin. Phys. B . 2018, 27(10): 107102 . **doi:** 10.1088/1674-1056/27/10/107102

Structural evolution and magnetic properties of $ScLi_n$ ($n = 2$–13) clusters: A PSO and DFT investigation*

Lu Li(栗潞)[1], Xiu-Hua Cui(崔秀花)[1,†], Hai-Bin Cao(曹海宾)[2], Yi Jiang(姜轶)[1], Hai-Ming Duan(段海明)[1], Qun Jing(井群)[1], Jing Liu(刘静)[1], and Qian Wang(王倩)[1,‡]

[1] School of Physical Science and Technology, Xinjiang University, Urumqi 830046, China
[2] Department of Physics, College of Sciences, Shihezi University, Shihezi 832000, China

(Received 12 January 2020; revised manuscript received 14 April 2020; accepted manuscript online 28 April 2020)

The stable geometries, electronic structures, and magnetic behaviors of the $ScLi_n$ ($n = 2$–13) clusters are investigated by using particle swarm optimization (PSO) and density functional theory (DFT). The results show that these clusters have three-dimensional (3D) structures except $ScLi_2$, and $ScLi_{12}$, and $ScLi_{13}$ that possess the cage-like structures. In analyses of the average binding energy, second-order difference of energy, and fragmentation energy, $ScLi_{12}$ cluster is identified as magnetic superatom. The magnetic moment for each of these clusters owns an oscillating curve of different cluster sizes, and their magnetic moments are further investigated using molecular orbitals and jellium model. Of $ScLi_n$ ($n = 2$–13) clusters, $ScLi_{12}$ has the largest spin magnetic moment (3 μ_B), and molecular orbitals of $ScLi_{12}$ can be described as $1S^2 1P^6 1D_\alpha^5 D_\beta^2$. Additionally, Mulliken population and AdNDP bonding analysis are discussed and the results reveal that the Sc atom and Li_n atoms make equal contribution to the total magnetic moment, and atomic charges transfer between Sc atoms and Li atoms.

Keywords: density functional theory, most stable geometry, magnetic moment

PACS: 71.15.Mb, 13.40.Em, 36.40.Cg, 36.40.Qv **DOI:** 10.1088/1674-1056/ab8d9e

1. Introduction

Since the development of cluster science, the physical and chemical properties of small-sized clusters including $ScAl_n$ ($n = 1$–8,12),[1] S_n^Q ($n = 3$–20, $Q = 0, -1$),[2] $AuSi_n^-$ ($n = 4$–12),[3] $RuGe_n^-$ ($n = 3$–12),[4] M_nC ($M =$ Li, Na, K, Rb, and Cs; $n = 1$–8),[5] and so on[6–11] have been receiving widespread attention. Among small-sized clusters, the transition metal clusters have been extensively studied due to their interesting magnetic properties. For the pure transition metal clusters (3d, 4d),[12–14] such as Mn_n clusters ($n = 2$–8),[15] the ground state geometries with different spins are different. Furthermore, doping is thought to be beneficial to increasing the stability and regulating the total magnetic moment. Wang *et al.* pointed out that coating magnetic clusters with gold can both enhance the net magnetic moment of $[Mn_{13}@Au_{20}]^-$ cluster and attenuate the magnetic moment of $[Co_{13}@Au_{20}]^-$ cluster.[16] Ge *et al.* reported that the reactive activities of Au_nSc_m clusters towards small molecules are higher than that of pure gold cluster and that the Au_4Sc_2 cluster has higher stability.[17]

Recently, attention has been paid to the study of transition metal-doped alkali metals. A strategy to obtain magnetic superatoms was proposed that the magnetic superatoms can be realized by making a transition metal atom locate on the central site of a composite cluster while the surrounding atoms are the alkali atoms.[18–21] A series of transition metal-doped clusters were presented, such as VLi_n ($n = 1$–13),[22] $ScNa_n$ ($n = 1$–12),[19] VNa_n ($n = 1$–12),[18] VCs_n ($n = 1$–12),[18] *etc.* And the electronic and magnetic properties of these clusters have been investigated by using the first-principles calculations. Previous investigation showed that the electronic states of small metal clusters can be grouped into electronic shell sequence 1S, 1P, 1D, ..., much like the way in atoms.[18–20,23,24] Unlike atomic orbitals, the electronic states of superatoms delocalized over the clusters, and the filling of orbitals do not usually exhibit Hund's rule.[19,20] Reveles *et al.*[18] found out that magnetic superatoms can be designed by appropriate combinations of localized and delocalized electrons in the valence space of a cluster, and took VNa_8, VCs_8, and $MnAu_{24}(SH)_{18}$ as illustrative examples. Zhang *et al.* pointed out that VLi_8 clusters are identified as a magnetic superatom with a jellium sphere electronic structure.[22] Pradhan *et al.*[25,26] studied Sc-, Ti-, and V-doped Na_n clusters in the gradient corrected DFT framework. Pradhan *et al.*[26] pointed out that $ScNa_{12}$, ScK_{12}, and $ScCs_{12}$ clusters each can attain a large spin moment and the addition of alkali atoms to a Sc atom can result in a large spin moment.

It is interesting to note that the first 3d transition-metal atom Sc owns a similar atomic radius to lithium, while to the best of our knowledge there is still no report about the electronic and magnetic structures of Sc–Li binary clusters. Lithium is the first alkali metal in the periodic table whose

*Project supported by the Natural Science Foundation of Xinjiang Uygur Autonomous Region, China (Grant Nos. 2018D01C079 and 2018D01C072).
†Corresponding author. E-mail: xjcxh0991@xju.edu.cn
‡Corresponding author. E-mail: wq@xju.edu.cn
© 2020 Chinese Physical Society and IOP Publishing Ltd

subshell of valence electrons is $1s^2 2s^1$. It has been attracting much attention due to its high power and capacity of rechargeable lithium batteries, and the very interesting physical properties of lithium clusters. Zhang *et al.* pointed out that VLi_8 clusters are identified as a magnetic superatom with a jellium sphere electronic structure.[22] Additionally, Li *et al.* reported that an alternative behavior of odd and even is found in $CuLi_n$'s magnetic moment (total or local), for which the clusters with odd number valence electrons show relatively large magnetic effects.[27]

In this paper, the authors investigate in detail the stable geometries and magnetic properties of small-sized $ScLi_n$ ($n = 1$–12) clusters. The low energy structures are evaluated by using the particle swarm optimization[28,29] along with the first-principles method. Based on the obtained lowest-energy structures, different growth behaviors and magnetic properties are found. The results show that the core-shell $ScLi_{12}$ cluster has a regular icosahedral configuration and owns relatively large stability which could be a good candidate for superatoms. The magnetic properties of these clusters can be explained by the jellium sphere model, whose molecular orbitals are in 1S1P1D sequence. The net spin magnetic moment of $ScLi_{12}$ cluster is 3 μ_B and its molecular orbital arrangement is $1S^2 1P^6 1D_\alpha^5 1D_\beta^2$.

2. Computational details

During the calculation, geometric optimization was performed by using the spin-polarized density functional theory (DFT) implemented in the Vienna *ab initio* simulation package (VASP).[30,31] And the projector augmented wave (PAW) pseudopotentials[32] were used to describe the interaction of valence electrons with the ionic nucleus. The exchange and correlation energies were illustrated by the Perde–Burke–Ernzerhof (PBE) formula of the spin-polarized generalized gradient approximation (GGA).[33] The plane-wave cutoff was established to be 300 eV. The $ScLi_n$ clusters were placed in a cubic super lattice of $12\times12\times12$ angstrom (for $n < 9$) and $15\times15\times15$ angstrom (for $n \geq 9$).

In order to find out the lowest energy structure of the $ScLi_n$ cluster, we used the CALYPSO[29,34–36] structure prediction method, which is a global minimum search of the free energy surface. It successfully predicted structures for various systems.[37–42] We ran 20 generations for $ScLi_n$ ($n = 2$–9) and 30 generations for $ScLi_n$ ($n = 10$–13). Each generation produces 20 and 30 structures for $n = 2$–9 and $n = 10$–13 respectively. The first generation was randomly generated. For the next generation, 80% of the structure was inherited from the previous generation, and the rest was randomly generated. Then, several structures with the lowest energy were selected as the initial structures, which were re-optimized with more accurate convergence precision. The convergence of the cluster structure was based on the force component less than 10^{-4} eV/Å and the total energy variation less than 10^{-5} eV. Subsequent analysis of the cluster structure was performed in the Gaussian09 software package.[43] Harmonic vibrational frequencies were calculated to confirm that the optimized geometry structure is truly minimum and their vibrational frequencies are no imaginary values. The Mulliken population analysis and Adaptive natural density partitioning (AdNDP)[44] bonding analysis were calculated in the Multiwfn program package.[45,46] The AdNDP orbitals were plotted by using the VMD software.[47]

3. Results and discussion

3.1. Most stable geometry

Using the method described above, hundreds of isomers of $ScLi_n$ ($n = 2$–13) clusters with different sizes are obtained. After checking in detail the energy of each isomer, the low-energy structures of $ScLi_n$ ($n = 2$–13) clusters are obtained. The obtained low-energy $ScLi_n$ ($n = 2$–13) clusters are shown in Fig. 1. As shown in Fig. 1, each isomer is denoted as nA, in which n is the number of Li atoms and A is the alphabet which states the energy sequence from the lowest-energy of each isomer. For example, 2a means the lowest-energy structure of $ScLi_2$ cluster.

As shown in Fig. 1, among the $ScLi_n$ ($n = 2$–13) clusters, only the $ScLi_2$ (2a, 2b, 2c) and 3c own planar geometry and the geometry of 2c isomer own more near-linear structural features. For $n \geq 3$, the lowest-energy structures have a three-dimensional (3D) configuration which is tetrahedral structure, while the isomer (3c) has a rhombic structure. The lowest energy $ScLi_4$ cluster is a slightly distorted triangular bipyramid with C_{2v} symmetry. The other two isomers 4b, and 4c are just slightly higher than 4a, even the 4c isomer in which the Sc atom at the apex of the pyramid is 0.16 eV higher than 4a. The ground-state geometry of $ScLi_5$ has C_{4v} symmetry, the Sc atom locates at the top of the octahedron configuration. The 5b isomer with the boat-like geometry is only 0.01 eV less stable than the 5a. The most stable geometry of $ScLi_6$ cluster is pentagonal bipyramid structure with C_{5v} point group, and the Sc atom locates at the vertex. 6b/6c is Li-atom-capped octahedron, which can be seen as one Li-atom capped on distorted 5a. For the $ScLi_7$ cluster of C_s symmetry, an Li atom is added to the $ScLi_6$ cluster with distorted pentagonal bipyramid structure. For the following configurations, from the $ScLi_8$ cluster to the $ScLi_{11}$ cluster, the lowest-lying energy structures have similar structures and the Sc atom is gradually surrounded by the Li atoms. Similar growth behaviors are also found in their metastable states. As shown in Fig. 1, 8c and 7a have similar configurations. From $ScLi_9$ to $ScLi_{11}$ cluster, the structure of the isomers is present as a semi-enclosed structure with centered Sc atom. When the sizes of $ScLi_n$ clusters go up to

10, their configurations present approximately boat-like structures, and the scandium atom locates on the deck. The ground-state structure of $ScLi_{11}$ is a bowl-type shape with C_{5v} symmetry, and the Sc atom is in the bowl. Noting that for the isomer of $ScLi_{11}$ cluster $11c$, its geometry looks like a complete closed core–shell polyhedron with Sc atom centered. The lowest energy structure of $ScLi_{12}$ and $ScLi_{13}$ clusters owns cage-like structure with C_i and C_2 symmetries respectively, and one Sc atom locates inside the cage. In general, with the increase of the number of lithium atoms, Sc atoms gradually fall into the cage structure formed by Li atoms. At $ScLi_{12}$, Sc atoms completely locate in the cage, forming a perfect cage structure.

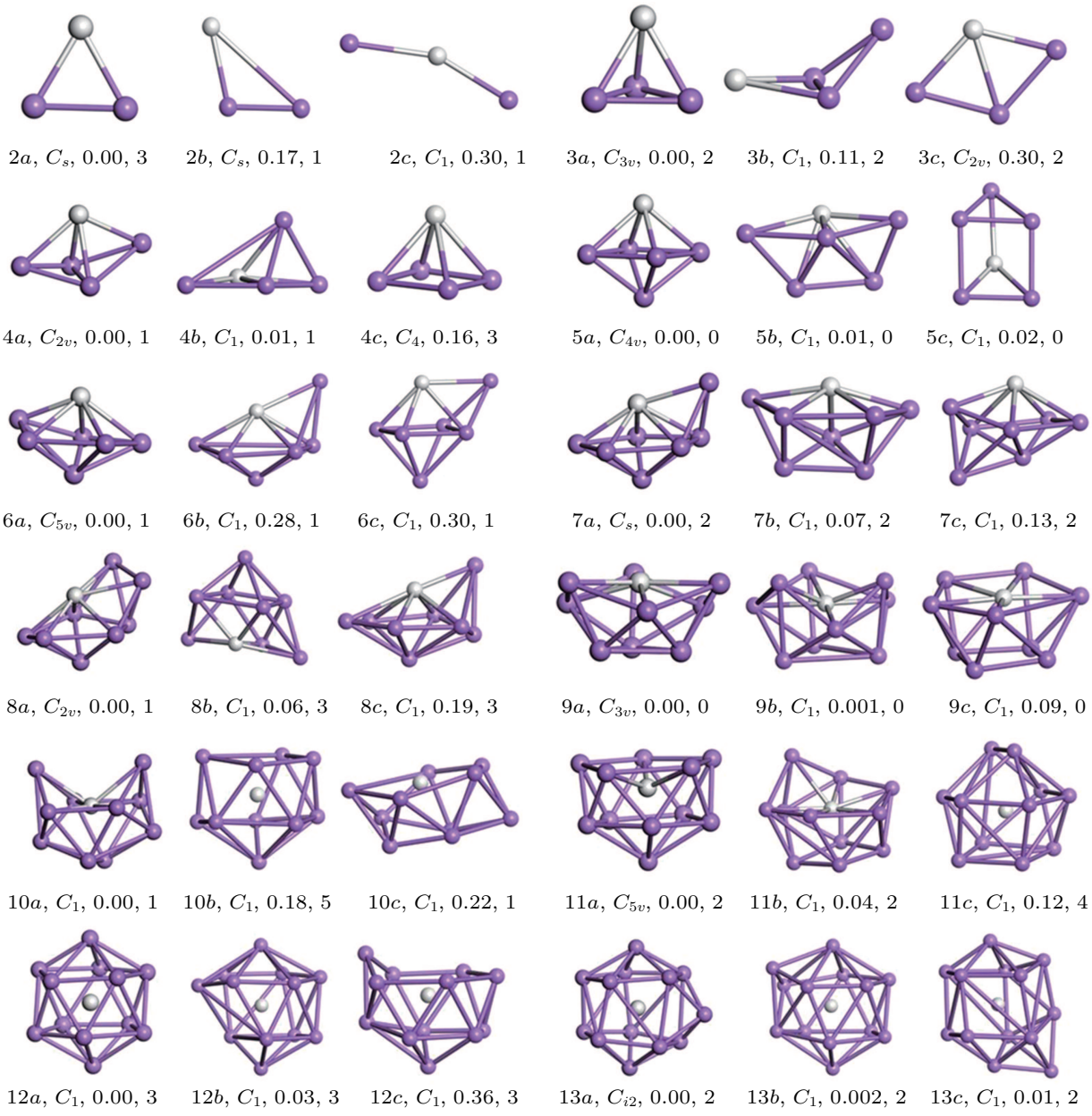


Fig. 1. Isomers of $ScLi_n$ ($n = 2$–13) clusters, with purple balls representing Li atoms and the gray ball denoting Sc atom.

3.2. Relative stabilities

The magic number of stable structure is very important for a cluster. Based on the obtained most stable geometry described above, the stabilities of these clusters are further evaluated by using their corresponding average binding energy (E_b), second-order energy difference ($\Delta^2 E$), and fragmentation energy (E_f), which are defined as follows:

$$E_b(\mathrm{ScLi}_n) = [nE(\mathrm{Li}) + E(\mathrm{Sc}) - E(\mathrm{ScLi}_n)]/(n+1), \quad (1)$$

$$\Delta^2 E(\mathrm{ScLi}_n) = E(\mathrm{ScLi}_{n+1}) + E(\mathrm{ScLi}_{n-1}) - 2E(\mathrm{ScLi}_n), \quad (2)$$

$$E_f(\mathrm{ScLi}_n) = E(\mathrm{ScLi}_{n-1}) + E(\mathrm{Li}) - E(\mathrm{ScLi}_n), \quad (3)$$

in which the E(Sc) and E(Li) are the energies of the isolated Sc atom and Li atom respectively, and the $E(\mathrm{ScLi}_{n-1})$, $E(\mathrm{ScLi}_n)$, and $E(\mathrm{ScLi}_{n+1})$ represent the total energies of the ScLi_{n-1}, ScLi_n, and ScLi_{n+1} clusters, respectively. The obtained values of average binding energy (E_b), the second-order energy difference ($\Delta^2 E$), and the fragmentation energy (E_f) are shown in

Fig. 2.

As shown in Fig. 2(a), one can find out that the average binding energy values of these clusters gradually are enhanced with the sizes of $ScLi_n$ clusters increasing until $n = 12$. After $n \geq 12$, the dependence of average binding energy on cluster size becomes smooth. From the data of average binding energy, one may deduce that the big size clusters with cage or cage-like geometry are more stable than those smaller sized clusters.

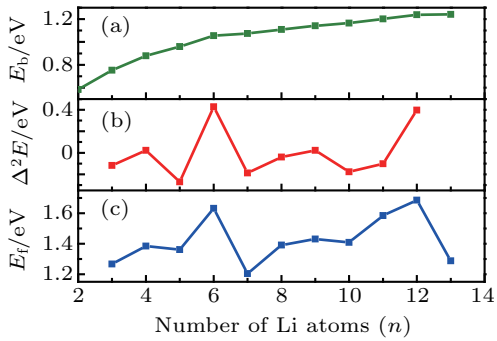


Fig. 2. (a) Average binding energy, (b) second-order energy difference, and (c) fragmentation energy of the lowest energy $ScLi_n$ ($n = 2$–13) clusters.

The second-order energy difference Δ^2E values of $ScLi_n$ clusters are plotted in Fig. 2(b). It is well shown that the Δ^2E is a sensitive factor reflecting the relative stability of adjacent size clusters. Figure 2(b) shows the fluctuation curve of Δ^2E *versus* the number of Li atoms for $ScLi_n$ clusters, and the local peaks that appear at $n = 6$, 9, 12, respectively, indicating that these clusters are more stable than their neighbor clusters.

To further probe the stabilities of the $ScLi_n$ clusters, we calculate the fragmentation energy (E_f) and the results are shown in Fig. 2(c). For the fragmentation energy (E_f) of $ScLi_n$ clusters, the trend of the curve is similar to second-order energy difference (Δ^2E). The high stability of $ScLi_6$ and $ScLi_{12}$ clusters are also found in the fragmentation energy (E_f).

In a word, comparison with the data shown in Fig. 2 shows that the $ScLi_{12}$ has relatively large stability in the $ScLi_n$ ($n = 2$–13) clusters.

3.3. Magnetic properties

It is interesting to investigate the magnetic properties of transition-metal atom doped alkali clusters such as VLi_n ($n = 1$–13),[22] $TiNa_n$ ($n = 1$–13),[21] $ScNa_n$ ($n = 4, 5, 6$),[25] VNa_n ($n = 4, 5, 6$)[25] clusters, *etc*. Based on the most stable geometries, the magnetic properties of the $ScLi_n$ ($n = 2$–13) clusters are investigated. The obtained magnetic moments of $ScLi_n$ clusters are shown in Fig. 3. As shown in Fig. 3, for $ScLi_n$ ($n = 2$–5), the magnetic moment of the cluster shows a downward trend until the magnetic moment is 0 μ_B, and then it increases to 2 μ_B (at $n = 5$–7) and decreases to 0 μ_B (at $n = 7$–9). For $ScLi_n$ ($n = 9$–12), the magnetic moment increases and reaches the maximum value of the magnetic moment at $ScLi_{12}$ (3 μ_B). The magnetic moment of the $ScLi_{13}$ cluster is reduced to 2 μ_B.

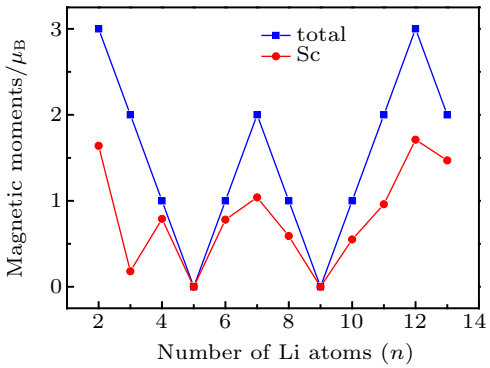


Fig. 3. Plots of magnetic moment *versus* Li atom number of $ScLi_n$ ($n = 2$–13) clusters and magnetic moment contribution made by Sc atoms.

Generally speaking, the orbitals of superatoms (clusters) own complex dependence on not only the valence electron but also the geometry due to the Jahn–Teller effect. The orbitals of superatoms may be explained by using the so-called jellium sphere modelsin which the electron shells can be represented by 1S, 1P, 1D, 2S, ... in a similar way to those by atomic orbitals (1s, 1p, 1d, ...), and the capital letters are used to separate them from atomic orbitals. In this paper, we investigate in detail the molecular orbitals of the most stable clusters by using the Gaussian 09 code. The obtained orbitals are shown in Fig. 4 and Figs. A1–A7 in Appendix A. Take $ScLi_{12}$ for example, it has 15 valence electrons (12 s electrons from the 12 Li atoms, and 3 electrons from the Sc atoms). From the molecular orbital shown in Fig. 4, one can find out that there are 9 α electrons and 6 β electrons, hence its net spin magnetic moments are 3 μ_B. After checking in detail the spatial characteristics of these molecular orbitals, we can find out that they own similar characteristics to the isolated atomic s, p, and d orbitals: the lowest two molecular orbitals should be s orbitals, and the next 6 orbitals between −3.8 eV and −4.6 eV are p orbitals, and the other 7 orbitals nearby −3 eV look like the d orbitals. According to the jellium model the molecular orbital of $ScLi_{12}$ can be described as $1\,S^2 1P^6 1D^5_\alpha 1D^2_\beta$.

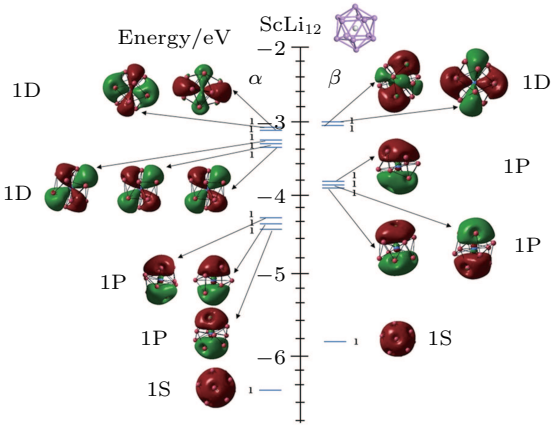


Fig. 4. Diagram of MOs and orbital energy level correlation of $ScLi_{12}$.

Using the jellium model described above, twe also investigate the molecular orbitals of the other $ScLi_n$ clusters. For $ScLi_n$ ($n = 2$–5) clusters which own about 5–8 valence electrons, the valence electrons are mainly 1S1P states: $1S^21P^3_\alpha$ ($n = 2$), $1S^21P^3_\alpha 1P^1_\beta$ (for $n = 3$), $1S^21P^3_\alpha 1P^2_\beta$ (for $n = 4$), and $1S^21P^6$ (for $n = 5$). So the net spin magnetic moments of these clusters decrease until no spin splitting is found for $n = 5$. From the $ScLi_6$ cluster, after one lithium atom is added, one more electron will be added into the molecule. The 1S state and 1P state have been fulfilled, hence the incremental electrons should locate in the 1D molecular states. Actually as shown in Figs. A1–A7 in Appendix A, the 1D states are found in $ScLi_n$ ($n = 6$–13) clusters. The increased magnetic moments each have a relation with the spin splitting of the 1D states in these clusters. For the $ScLi_6$ cluster, the molecular orbital is arranged as $1S^21P^61D^1_\alpha$. For the $ScLi_7$, as shown in Fig. A2 in Appendix A, the arrangement is $1S^21P^61D^2_\alpha$, and the magnetic moment is 2 μ_B. As for the $ScLi_8$ cluster (shown in Fig. A3 in Appendix A), the increasing tendency of the magnetic moment is broken off. The molecular orbital of $ScLi_8$ is $1S^21P^61D^2_\alpha D^1_\beta$, and its magnetic moment is 1 μ_B. We check in detail the unoccupied molecular orbital of the $ScLi_7$ cluster again, and find out that its α-LUMO (lowest unoccupied molecular orbital) energy is -1.6377 eV and β-LUMO energy is -1.7802 eV. The β-LUMO energy is lower, and the difference is about 0.14 eV. Hence once one Li atom is added to $ScLi_7$ cluster, the added valence electron will be put in the β-LUMO state, which makes the $ScLi_8$ cluster own the orbitals as $1S^21P^61D^2_\alpha 1D^1_\beta$. As for the $ScLi_9$ cluster (shown in Fig. A4 in Appendix A), it is like $ScLi_5$ cluster whose magnetic moment is 0 μ_B, and the molecular orbital arrangement is $1S^21P^61D^2_\alpha 1D^2_\beta$. The molecular orbital arrangement of $ScLi_{10}$ (Fig. A5) is $1S^21P^61D^3_\alpha D^2_\beta$. We can further study the magnetic moment changes of $ScLi_{11}$ cluster. The energy of α-LUMO of $ScLi_{10}$ is -1.8738 eV, the energy of β-LUMO of $ScLi_{10}$ is -1.8128 eV, the α-LUMO energy is obviously lower: their difference is about 0.06 eV. Therefore, after adding one Li atom, the added valence electron locates in the α-LUMO state, which makes the orbit of the $ScLi_{11}$ cluster $1S^21P^61D^4_\alpha 1D^2_\beta$. Similarly, we can obtain the arrangement of $ScLi_{12}$ cluster, the energy of α-LUMO (-1.8846 eV) is lower than that of β-LUMO (-1.8381 eV) in $ScLi_{11}$ cluster, which makes the $ScLi_{12}$ cluster own the orbitals as $1S^21P^61D^5_\alpha D^2_\beta$. In addition, the energy of β-LUMO (-1.9366 eV) is less than that of α-LUMO (-1.8512 eV) in $ScLi_{12}$ cluster, hence the $ScLi_{13}$ cluster owns the orbitals as $1S^21P^61D^5_\alpha D^3_\beta$.

To better understand the atomic contribution to the total magnetic moment of each of $ScLi_n$ clusters, the Mulliken population analysis is further performed by using the Multiwfn software. The obtained atomic magnetic moment is shown in Fig. 3 and Table A1 in Appendix A. As shown in Fig. 3, one can find out that the atomic magnetic moment of Sc owns a similar tendency to the total magnetic moment of $ScLi_n$ clusters, but it is smaller than total magnetic moment, especially for $ScLi_2$, $ScLi_3$, and $ScLi_{7-12}$. As shown in Table A1 in Appendix A, the atomic magnetic moments for Sc atom and Li atom are 1.64 and 1.36 (for ScLi2), 0.18 and 1.82 (for $ScLi_3$), 1.04 and 0.96 (for $ScLi_7$), 0.59 and 0.41 (for $ScLi_8$), 0.55 and 0.45 (for $ScLi_{10}$), 0.96 and 1.04 (for $ScLi_{11}$), and 1.71 and 1.29 (for $ScLi_{12}$). That is to say, the Sc atom and Li_n atoms make equal contribution to the total magnetic moment.

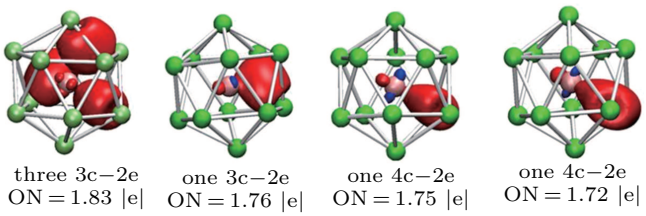


Fig. 5. AdNDP analysis results of $ScLi_{12}$ cluster. Ideal value of occupation number (ON) is 2.00 |e|.

The chemical bond and atomic charges are further investigated. Hereafter, we just take $ScLi_{12}$ for example. The chemical bond, atomic charges of other $ScLi_n$ clusters are similar to those of the $ScLi_{12}$ cluster. The chemical bonding analysis of the $ScLi_{12}$ cluster is performed by using the AdNDP method, which can explain the bonding of a cluster in accordance with n-center two-electron (nc−2e) bonds ($1 \leq n \leq$ total number of atoms of the system). As shown in Fig. 5, the $ScLi_{12}$ cluster contains 6 delocalized bonds, ordered by occupation number (ON) ranging from 1.72 |e| to 1.83 |e|. There are included 6 delocalized bonds, *i.e.*, four 3c–2e bonds and two 4c–2e bonds. Using the Mulliken population analysis, we also check the atomic charges of Sc atom and Li atom in $ScLi_{12}$ cluster. The obtained atomic charges of Sc, and Li atoms are -5.40 e, and 0.43 e–0.47 e, respectively. That is to say, due to the interaction between Sc and Li atoms, the atomic charges transfer from Li atoms to Sc atoms. After check in detail the atomic charge population, one can also find out that for the Sc atom, the atomic charges of Sc-s, Sc-p, Sc-d states are 6.76 e, 18.22 e, and 1.42 e, respectively. As for Li atoms, the atomic charges of Li-s state and Li-p state are ~ 2.10 e and ~ 0.42 e, respectively. Hence the atomic charges are transferred from Li-s state to Li-p state, and Sc atoms. The atomic spin population shows that the spin population of Sc-s, Sc-p, and Sc-d states are 0.00, 0.95, and 0.74 respectively, and the spin population of Li-s and Li-p states are ~ 0.04, and ~ 0.08 respectively. The total magnetic moment of all 12 Li atoms are then about 1.30. In a word, due to the delocalized chemical bond between Sc and Li atoms, the atomic charges are transferred

from Li atom to Sc atom, which leads the Li atom and Sc atom to make nearly equal contributions to the total magnetic moment.

4. Conclusions

In this paper, the stable geometries, the electronic structures and magnetic properties of $ScLi_n$ ($n = 2$–13) clusters are investigated by using the PSO method (implemented in the CALYPSO code) and DFT method. The results show that all of the $ScLi_n$ ($n = 2$–13) clusters prefer to take 3D structures except $ScLi_2$. Among these $ScLi_n$ clusters, the $ScLi_{12}$ and $ScLi_{13}$ have cage configurations, and the $ScLi_{12}$ cluster presents a perfect icosahedral structure. After checking in detail the average binding energy, the second-order energy difference, and the fragmentation energy, the $ScLi_{12}$ cluster is thought to be the magnetic superatom. The magnetic moments of $ScLi_n$ ($n = 2$–13) clusters each own an oscillating curve with different cluster sizes. The magnetic behaviors of these clusters can be explained by using the so-called jellium sphere model whose subshells of molecular orbital can be described as 1S1P1D ... in the way in isolated atoms. And the $ScLi_{12}$ has the largest spin magnetic moment (3 μ_B), and the molecular orbital of $ScLi_{12}$ can be described as $1S^2 1P^6 1D_\alpha^5 D_\beta^2$. The atomic charges are transferred from Li atom to Sc atom in the $ScLi_{12}$ cluster, which leads the Li atom and Sc atom to make nearly equal contribution to the total magnetic moment. It is supported by the Mulliken population and AdNDP bonding analysis.

Appendix A: Supporting information

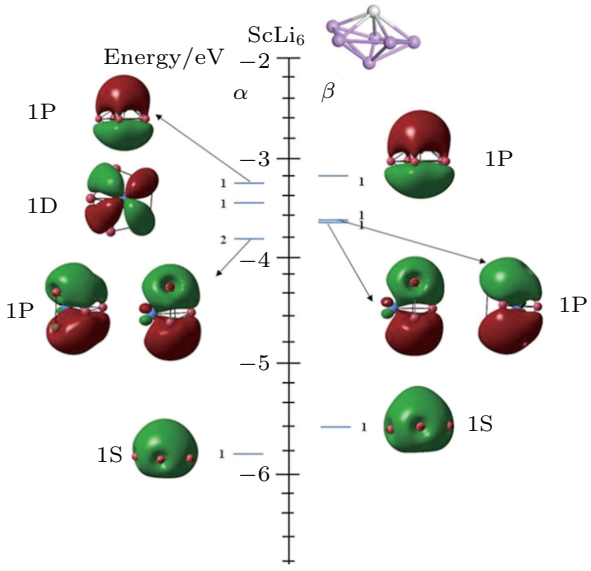


Fig. A1. MOs of $ScLi_6$ cluster.

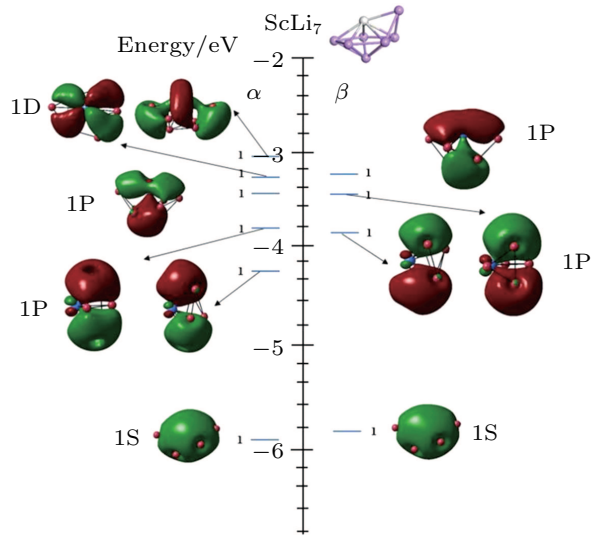


Fig. A2. MOs of $ScLi_7$ cluster.

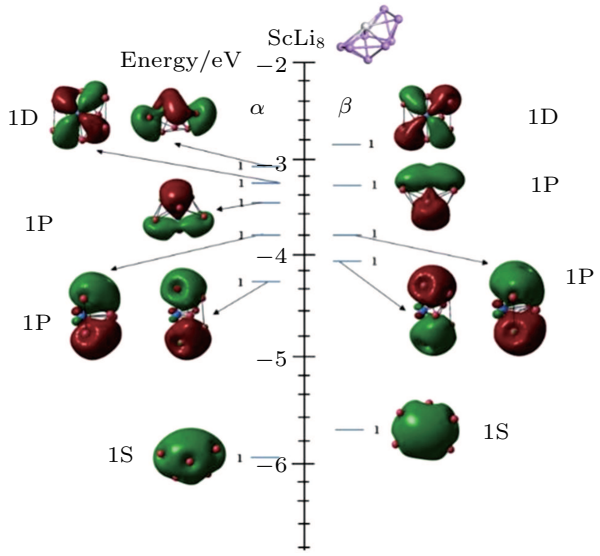


Fig. A3. MOs of $ScLi_8$ cluster.

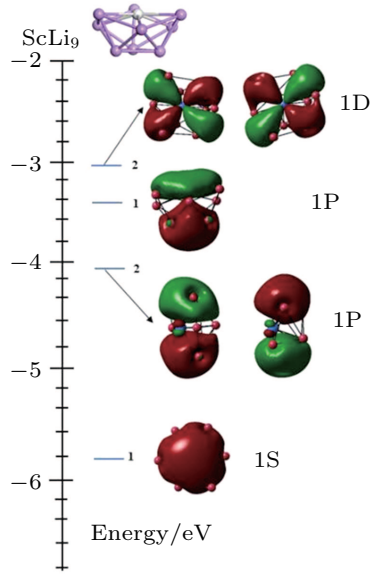


Fig. A4. MOs of $ScLi_9$ cluster.

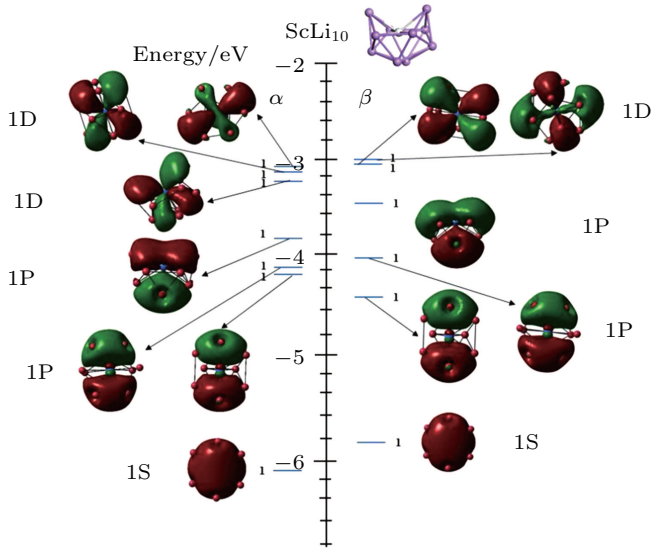


Fig. A5. MOs of $ScLi_{10}$ cluster.

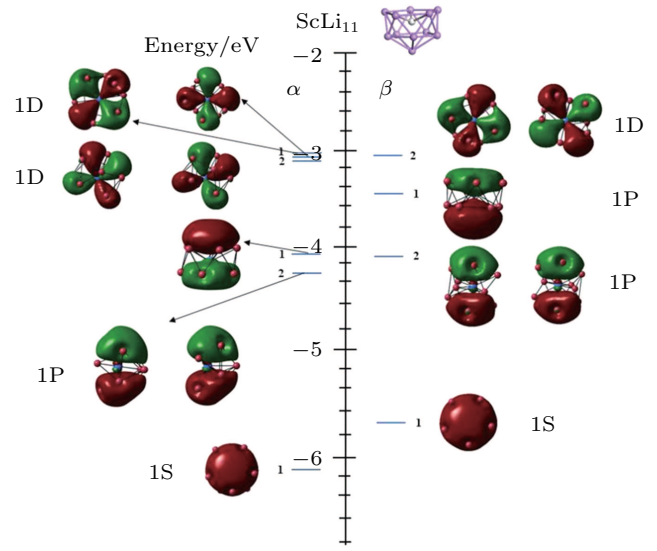


Fig. A6. MOs of $ScLi_{11}$ cluster.

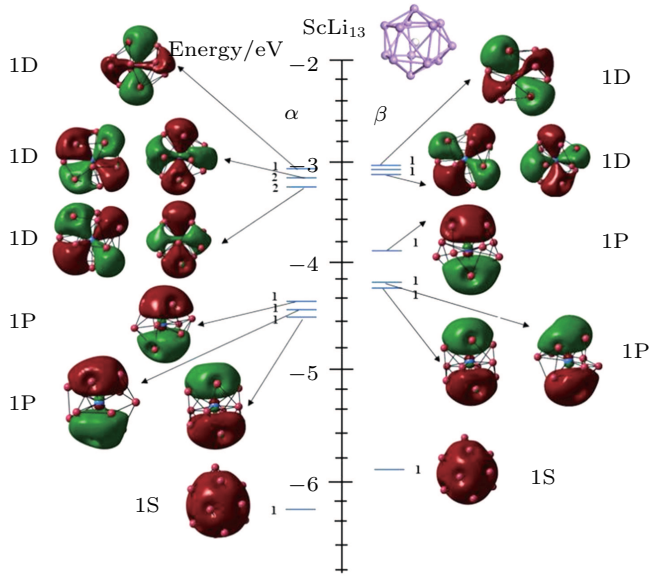


Fig. A7. MOs of $ScLi_{13}$ cluster.

Table 1. Contribution of atoms in $ScLi_n$ cluster to spin magnetic moment by Mulliken population analysis.

$ScLi_n$	Total	Sc	Li_n
$ScLi_2$	3	1.64	1.36
$ScLi_3$	2	0.18	1.82
$ScLi_4$	1	0.79	0.21
$ScLi_5$	0	0	0
$ScLi_6$	1	0.78	0.22
$ScLi_7$	2	1.04	0.96
$ScLi_8$	1	0.59	0.41
$ScLi_9$	0	0	0
$ScLi_{10}$	1	0.55	0.45
$ScLi_{11}$	2	0.96	1.04
$ScLi_{12}$	3	1.71	1.29
$ScLi_{13}$	2	1.47	0.53

References

[1] Tian F Y, Jing Q and Wang Y X 2008 *Phys. Rev. A* **77** 013202
[2] Jin Y Y, Maroulis G, Kuang X Y, Ding L P, Lu C, Wang J J, Lv J, Zhang C Z and Ju M 2015 *Phys. Chem. Chem. Phys.* **17** 13590
[3] Lu S J, Xu X L, Feng G, Xu H G, Zheng and W J 2016 *J. Phys. Chem. C* **120** 25628
[4] Jin Y, Lu S, Hermann A, Kuang X, Zhang C, Lu C, Xu H and Zheng W 2016 *Sci. Rep.* **6** 30116
[5] Shao P, Chen B L, Ding L P, Luo D B, Lu C and Kuang X Y 2017 *Phys. Chem. Chem. Phys.* **19** 25289
[6] Lu S J 2019 *Phys. Chem. Chem. Phys.* **21** 26154
[7] Xiong R, Die D, Xiao L, Xu Y G and Shen X Y 2017 *Nanoscale Res. Lett.* **12** 625
[8] Zhao Y R, Bai T T, Jia L N, Xin W, Hu Y F, Zheng X S and Hou S T 2019 *J. Phys. Chem. C* **123** 28561
[9] Kang D, Sun W, Shi H, Lu C, Kuang X, Chen B, Xia X and Maroulis G 2019 *Sci. Rep.* **9** 14367
[10] Jing Q, Ge G X, Cao H B, Huang X C, Liu X Y and Yan H X 2010 *Acta Phys. Chim. Sin.* **26** 2510
[11] Jing Q, Tian F Y and Wang Y X 2008 *J. Chem. Phys.* **128** 124319
[12] Gong X G and Zheng Q Q 1995 *Phys. Rev. B* **52** 4756
[13] Akola J, Walter M, Whetten R L, Hakkinen H and Gronbeck H 2008 *J. Am. Chem. Soc.* **130** 3756
[14] Das A, Li T, Nobusada K, Zeng Q, Rosi N L and Jin R 2012 *J. Am. Chem. Soc.* **134** 20286
[15] Pederson M R, Reuse F and Khanna S N 1998 *Phys. Rev. B* **58** 5632
[16] Wang J, Bai J, Jellinek J and Zeng X C 2007 *J. Am. Chem. Soc.* **129** 4110
[17] Ge G X, Yan H X, Jing Q, Huang X M, Wan J G and Wang G H 2013 *Eur. Phys. J. D* **67** 116
[18] Reveles J U, Clayborne P A, Reber A C, Khanna S N, Pradhan K, Sen P and Pederson M R 2009 *Nat. Chem.* **1** 310
[19] Pradhan K, Reveles J U, Sen P and Khanna S N 2010 *J. Chem. Phys.* **132** 124302
[20] Medel Juarez V, Reveles J, Khanna S, Chauhan V, Sen P and Castleman A 2011 *Proc. Nat. Acad. Sci. USA* **108** 10062
[21] Reveles J, Sen P, Pradhan K, Roy D and Khanna S 2010 *J. Phys. Chem. C* **114** 10739
[22] Zhang M, Zhang J, Feng X, Zhang H, Zhao L, Luo Y and Cao W 2013 *J. Phys. Chem. A* **117** 13025
[23] Castleman A W and Khanna S N 2009 *J. Phys. Chem. C* **113** 2664
[24] Walter M, Akola J, Acevedo O L, Jadzinsky P, Calero G, Ackerson C, Whetten R, Grönbeck H and Häkkinen H 2008 *Proc. Nat. Acad. Sci. USA* **105** 9157
[25] Pradhan K, Sen P, Reveles J and Khanna S 2008 *Phys. Rev. B* **77** 045408
[26] Pradhan K, Reveles J U, Sen P and Khanna S N 2010 *J. Chem. Phys.* **132** 124302
[27] Wang Y, Lv J, Li Q, Wang H and Ma Y 2019 *CALYPSO Method for Structure Prediction and Its Applications to Materials Discovery*, in *Handbook of Materials Modeling*, eds. Andreoni W and Yip S (Cham: Springer)
[28] Lv J, Wang Y, Zhu L and Ma Y 2012 *J. Chem. Phys.* **137** 084104

[29] Wang Y, Lv J, Zhu L and Ma Y 2012 *Comput. Phys. Commun.* **183** 2063
[30] Kresse G and Furthmüller J 1996 *Comput. Mater. Sci.* **6** 15
[31] Kresse G and Furthmüller J 1996 *Phys. Rev. B* **54** 11169
[32] Kresse G and Joubert D 1999 *Phys. Rev. B* **59** 1758
[33] Perdew J P, Chevary J A, Vosko S H, Jackson K A, Pederson M R, Singh D J and Fiolhais C 1992 *Phys. Rev. B* **46** 6671
[34] Wang Y, Miao M, Lv J, Zhu L, Yin K, Liu H and Ma Y 2012 *J. Chem. Phys.* **137** 224108
[35] Lv J, Wang Y, Zhu L and Ma Y 2012 *J. Chem. Phys.* **137** 084104
[36] Wang Y, Lv J, Zhu L and Ma Y 2010 *Phys. Rev. B* **82** 094116
[37] Wang Y, Lv J, Li Q, Wang H and Ma Y 2018 *Handbook of Materials Modeling: Applications: Current and Emerging Materials*, eds. Andreoni W and Yip S (Cham: Springer International Publishing) **1** 28
[38] Luo X, Yang J, Liu H, Wu X, Wang Y, Ma Y, Wei S H, Gong X and Xiang H 2011 *J. Am. Chem. Soc.* **133** 16285
[39] Zhang X, Wang Y, Lv J, Zhu C, Li Q, Zhang M, Li Q and Ma Y 2013 *J. Chem. Phys.* **138** 114101
[40] Lu S, Wang Y, Liu H, Miao M S and Ma Y 2014 *Nat. Commun.* **5** 3666
[41] Dong X, Jalife S, Vasquez-Espinal A, Ravell E, Pan S, Cabellos J L, Liang W Y, Cui Z H and Merino G 2018 *Angew. Chem. Int. Ed. Engl.* **57** 4627
[42] Le Chen B, Sun W G, Kuang X Y, Lu C, Xia X X, Shi H X and Maroulis G 2018 *Inorg. Chem.* **57** 343
[43] Frisch M J, Trucks G W, Schlegel H B, *et al*. 2013 *Gaussian 09*, Revision E.01, Gaussian, Inc., Wallingford CT
[44] Zubarev D Y and Boldyrev A I 2008 *Boldyrev. Phys. Chem. Chem. Phys.* **10** 5207
[45] Tian Lu and Feiwu Chen 2012 *J. Comput. Chem.* **33** 580
[46] Tian L and Chen F W 2011 *Acta Chim. Sin.* **69** 2393 (Chinese)
[47] Humphrey W, Dalke A and Schulten K 1996 *J. Mol. Graph.* **14** 33